PNAS

Supporting Information for

Pre-meiotic pairing of homologous chromosomes during Drosophila male meiosis

Thomas Rubin, Nicolas Macaisne, Ana Maria Vallés, Clara Guilleman, Isabelle Gaugué, Laurine Dal Toe and Jean-René Huynh

Jean-René Huynh
Email: jean-rene.huynh@college-de-france.fr

This PDF file includes:

Supporting text
Figures S1 to S10
Tables S1 to S6
Legends for Movies S1 to S8
SI References

Other supporting materials for this manuscript include the following:

Movies S1 to S8

Supporting Information Text

Experimental Model and Subject Details

Drosophila melanogaster

Flies were maintained on standard medium in 25°C incubators on a 12 h light/dark cycle. All koi rescue experiments were carried out at 29°C. Wild-type controls alone and in combination with additional transgenes of fluorescently tagged proteins were in a w^{1118} background. The shRNA for white was used as control for knock-down experiments because white is not expressed during oogenesis and spermatogenesis.

Fly stocks and genetics

For testing mutants, the following strains were used: $c(3)G^{68}$ (29), $c(3)^{G1}$ (BDSC: 606), $c(3)G^{G5001}$ (BDSC: 30110), $cona^{A12}/cona^{f04903}$(1), koi^{80}((2) BDSC: 25105), $klar^{mCD4}$ ((3) BDSC: 25097), $Dhc64c^{3-2}/Dhc64c^{6-12}$ (4), ord^{1} (BDSC:1433); ord^{10} (5).

The c(3)G deficiencies were : *Df(3R)BSC569* (BDSC: 25670), *Df(3R)ED5705* (BDSC: 9152). The shRNA lines were: for *white*, P{TRiP.GL00094}attP2 (BDSC: 35573); for *CdK1/cdc2* P{TRiP.GL00262}attP2 (BDSC: 35350); for *CycB* P{TRiP.HMS01015}attP2 (BDSC: 34544), for *twine* P{TRiP.HMS00642} (BDSC: 3044), for *c(3)G* P{TRiP.HMJ30046} (BDSC: 62969); for *tef* P{TRiP.GLV21094} (BDSC: 37488), for *ord* P{TRiP.HMJ22248} (BDSC: 58228), for mod(mdg4) P P{TRiP.HMS00795}(BDSC: 32995), for *sunn* P{TRiP.HMJ21654} (BDSC: 52969. P{bam-GAL4:VP16} (a gift from M. Fuller, Stanford University School of Medicine, CA, USA, and P{GAL4::VP16-nos.UTR} (BDSC 4937) were used as driver.

Live-imaging experiments were done using: CID::RFP (6), Mud::GFP (7), protein trap Koi::GFP (y[1] w[*]; P{w[+mC]=PTT-GB} koi[CB04483], BDSC: 51525); svv::GFP (8) and tmod::GFP (9); Nup107-GFP (10); HipHop::GFP (11)

For sperm exhaustion assays, single males were mated to two wild-type w^{1118} females. The males were aspirated without anesthetizing into new vials containing two fresh females every three days for 18 days. Fertility was assessed by scoring the number of progeny that hatched over 8 days.

Nondisjunction Tests

Sex chromosome nondisjunction was monitored by scoring the progeny of *y/BS Y* males carrying meiotic mutations on the second and/or third chromosome mated to w females. For crosses with RNAi lines, the nosGAL4 driver was used. In most cases, a male to female ratio of 5:10 was kept. From these crosses, *diplo-X* and *nullo-X* exceptions resulting from sex chromosome nondisjunction and normal gametes are obtained. Frequency of nondisjunction was calculated from the percentage of exceptional progeny obtained and compared to the control.

To determine autosomal 2nd chromosome nondisjunction, males carrying the meiotic mutations were mated to *C(2)EN b pr* (BDSC: 1112) females and the number of progeny scored. For crosses with RNAi lines, the nosGAL4 driver was used. In most cases, a male to female ratio of 5:10 was kept. From these crosses, only the exceptional *diplo-2* and *nullo-2* gametes are observed. Frequency of nondisjunction was calculated as the number of exceptional progeny over the number of males crossed and compared to the control.

RNA extraction from ovaries and testis

For RT-qPCR, w^{1118} flies were used. Ovaries and testis were dissected and collected in cold PBS. Tissues were homogenized with a pestle and RNA was extracted following the standard protocol from the RNeasy Micro Kit (QIAGEN).

RT–qPCR

cDNA was prepared from 0.5 µg total RNA following standard manufacturer's protocol using random primers, 10 mM dNTP mix, 5X first strand buffer, 0.1 M DTT, 40 U RNaseOUT, 200 U SuperScript III RT (Invitrogen). Typically, 10% of the reaction was used as template. Real time PCR was carried out using SYBR Green Supermix (Bio-Rad) with a Roche LightCycler II 480. Cycle threshold (C (T)) values were determined by the software. Calculation of relative RNA levels were done using the 2[-ΔΔ C (T)] method (12), where the C (T) values were normalized to those of rp49 in the same sample. Values used where the means of triplicate repeats.
Primers used in this study are:

hth: F 5' AGCAAAGGCTTCCCAATACA 3'; R 5' CCGTGTGGAGTCCTTAGATTTAC3'

bam: F 5' CTGCATATGATTGGTCTGCACGGC 3'; R5'CCCAAATCGGCGGTCAGGTGATC 3'

c(3)G: F 5' TAACTGCCTGATCGACCAAC 3'; R 5' TTTCCGGTTGCACCTTAGTAG 3'

cona: F 5'ATGTCCTGATTGCCGAGAAG 3'; R 5' GGATCTTGGCGTTCTTCGTAT 3'

rp49: F 5' ATCTCGCCGCAGTAAACGC 3'; R 5' CCGCTTCAAGGGACAGTATCTG 3'

Immunohistochemistry

For confocal microscopy, testis and ovaries were dissected in PBS, fixed in 4% PFA–PBS, and then permeabilized in PBT (0.2% Triton) for 30 min. Samples were incubated overnight with primary antibodies in PBT at 4 °C, washed 4 × 30 min in PBT, incubated with secondary antibody for 2 h at room temperature, washed 4 × 30 min in PBT. DAPI (1:500) was added during the last wash and then mounted in CityFluor.

For STED and Airyscan microscopy, testes were dissected in PBS, fixed in 4% PFA–PBS, permeabilized in PBT (0.2% Triton) for 30 min, then in PBT (0,4% Triton) + 10% BSA) for 1 hour. Samples were incubated for 72 hours with primary antibodies at 4 °C, washed 4 × 30 min in PBT,

incubated with secondary antibody for 2 h at room temperature, washed 4 × 30 min in PBT. DAPI (1:500) was added during the last wash and then mounted in CityFluor.
For TUNEL experiments, testes were dissected in PBS, fixed in 4% PFA-PBS, permeabilized in PBT (0.2% Triton) for 20 min and then TUNEL labeling was carried out using the In situ cell death Detection Kit, Fluorescein (Roche). TUNEL reaction mixture (8 µl Enzyme solution and 72 µl of Label solution per sample) was incubated overnight at 4°C, then washed 8 x 15 min in PBT. DAPI (1:500) was added during the last wash and then mounted in CitiFluor.
For FISH experiments, testes were dissected in PBS, fixed in 4% PFA in 1X fix buffer (100 mm potassium cacodylate, 100 mm sucrose, 40 mm sodium acetate, and 10 mm EGTA). Testes were then rinsed three times in 2X SSCT and incubated with the AACAC and dodeca probes which target the pericentromeric regions of the 2nd and 3rd chromosome, respectively, as previously described (13). Testes were then rinsed in 2X SSCT, twice in PBST and process for immunostaining as described above for confocal microscopy.
The following primary antibodies were used: mouse anti-C(3)G 1A8-1G2 (1:500) (gift from S. Hawley, Stowers Institute, USA), rat anti-Cid (1:1,000) (gift from C. E. Sunkel, Universidade do Porto, Portugal), rabbit anti-α-Spectrin (1:1,000 and 1:500 when used with FISH) (gift from R. Dubreuil, University of Chicago, USA), rat anti-Klaroid (1:200), guinea pig anti-Klarsicht (1:200) (gifts from M. Welte, University of Rochester, USA and J. Fischer, University of Texas, USA). Mouse anti α-tubulin DM1A (SIGMA) (1:500).
Secondary antibodies conjugated with Cy3, Cy5, FITC (Jackson laboratories) and STAR RED (abberior) were all used at 1:200.

Colcemid treatments.

Colcemid was prepared at a concentration of 0.2 mg ml−1 in 1% saccharose, mixed with dry yeast and then added to the fly medium. To assay pairing and clustering of centromeres in fixed samples, long-term drug treatments lasted 48 h. Freshly prepared drug was added every 12 h. For live-imaging, adult flies were fed for four hours with colcemid-containing media. Live-imaging was performed as described below.
We also analyzed the different classes of CID number categories in the 8cc after 3 cell divisions. We did not detect new classes under 3 CID dots as in WT nor an increase in 8 or more CID dots (Figure S10), suggesting that colcemid treatment did not alter germline cells divisions and chromosome number.

Image acquisition

Live and fixed imaging of testes and ovaries was done from 3-5 day-old flies.
For fast acquisitions of centromeres, all dissections were done in oil (10S, Voltalef, VWR). The muscular sheath around each ovariole was removed and germaria were made to stick to

coverslips. Live-imaging was done using an inverted spinning-disc confocal microscope (Roper/Nikon) operated by Metamorph software on an inverted Nikon Eclipse Ti microscope coupled to an Evolve EMCCD camera (Photometrics). All images were acquired with the PlanApo 60×/1.4 NA Oil objective with ×1.5 auxiliary magnification. Single-position videos in testis and germarium were acquired for 8 min at 25 ± 1 °C, with a 10 s temporal resolution (11-slice Z-stack, 0.5 µm per slice).

For long cell cycle live imaging of females versus males, ovaries and testis were dissected in Schneider medium (Sigma-Aldrich) supplemented with 15% fetal calf serum and 0.6% penicillin-streptomycin (Invitrogen). Muscle sheath from germaria was manually removed. Several *w*^{1118}; *svv::GFP/+; tmod::GFP/+* testis and ovarioles were each placed in a small drop of Growth Factor Reduced Matrigel (Corning) on a glass coverslip culture dish (P35G-1.0-14-C MatTeck), filled with medium, covered with a gas permeable membrane, and sealed with oil. Imaging was performed using a DeltaVision (Applied Precision) microscope system equipped with an Olympus 1670 inverted microscope and a CoolSNAP HQ CCD 40x1.42 camera. Confocal images (55 sections of 1.3 um per time point) were collected every 10 minutes. Tracking of cells was done manually using Fiji (ImageJ) processing program.

For cell cycle rescue live-imaging, a protocol adapted from (14) was used. *w ; svvGFP; bam>shRNA* ovaries were dissected in supplemented Schneider medium, and transferred onto a round 25 mm coverslip previously coated with 3-(trimethoxysilyl) propyl methacrylate (Sigma-Aldrich). Medium was then replaced with 10% PEG-DA hydrogel solution (esibio) containing 0.1% I2959 (photoinitiator, Sigma-Aldrich). Another coverslip treated with water repellent (Rain-X) was placed over the hydrogel droplet. The cover-slip/coverslip sandwich was then exposed to a UV Transilluminator for 30 s (312 nm) for gelation. The upper coverslip was then removed and the lower coverslip supporting the hydrogel disc placed into a Chamlide chamber filled with medium (14). Videos were collected with an inverted spinning-disc confocal microscope (Roper/Nikon) operated by Metamorph on an inverted Nikon Eclipse Ti microscope coupled to an Evolve EMCCD camera (Photometrics). All images were acquired with a PlanApo 60×/1.4 NA oil objective with ×1.5 auxiliary magnification. Single-position videos were acquired for 8 min, with a 10 s temporal resolution (11-slice Z-stack, 0.5 µm per slice). All images were acquired at 29°C.

Confocal images of fixed germaria and testes were obtained with a Zeiss LSM 980 NLO confocal. All images were acquired with a PlanApo 63×/1.40 NA oil objective at 0.5 µm intervals along the z-axis operated by ZEN 2012 software.

Super-resolution STED imaging was performed with a STEDyCON (Abberior Instruments) mounted at the camera port of an AxioObserver (Zeiss) microscope equipped with a 100 × objective (APO 100x/1.4 NA Oil). Star Red was imaged with excitation wavelength of 640 nm and time-gated fluorescence detection between 650 and 720 nm. The STED laser wavelength

of 775 nm and a pulse width of ~ 1–7 ns were used. The pinhole was set to 1.13 AU. The images were further processed (black/white inversion) with the Fiji software 103.
Phase-contrast micrographs of postmeiotic spermatids were done using live testes squashed examined under a Leica DMIRBE inverted microscope equipped with a 63X objective coupled to a CCD coolsnapHQ (Roper Scientific) operated by Metamorph software.

Data analysis

For quantification of CID foci on fixed tissue, we counted the number of distinguishable CID foci within each single nucleus. For quantification in live tissue, we consider all CID foci at a given (t) projection where the number of CID foci was maximal. In all figures, micrographs represent the projections of selected z-series taken from the first CID foci signal until the last one. For FISH experiments, the 3D distances between the AACAC foci and between the dodeca foci were measured as described (13). Pericentromeric regions of chromosomes were considered as paired when only one foci was visible or when two foci were separated by a distance less than 0.70 µm, and as unpaired when ≥ 0.70 µm. To assign the number of CID dots to a cyst developmental stage, we used α-Spectrin immunolabelling in fixed tissue and live MUD::GFP expression.
Three-dimensional tracking of CID foci was performed using Imaris software (Bitplane). The CID::RFP signal was tracked using the 'spots' function with an expected diameter of 0.6 µm. Automatically generated tracks were edited manually to eliminate inappropriate connections (e.g. connections between foci in different nuclei or between foci of different sizes or intensity, multiple assignments or multiple spots assigned to the same focus). To remove global movements of the germarium, each nucleus containing a CID::RFP focus was assigned to the nearest fusome. Then, the position of the reference fusome was subtracted from each CID::RFP focus for each time point to obtain the relative tracks. These relative tracks were then compiled using a custom MATLAB (MathWorks) routine that computes the minimum volume of the ellipsoid that encloses all of the three-dimensional points of the trajectory.

Analysis of centromere trajectories

Positions of individual centromeres were tracked every 10 s during 8 min to quantify the volume covered by each centromere. This raw volume was then corrected both for overall movements of the tissue and for variations in total nuclear volume. First, we subtracted the motion of the germarium using the position of the fusome as a reference within each cyst (Figure 4E). Second, to take into account the significant decrease of the nuclear volume from GSCs to 16-cell cysts (see Figure S9A), we computed the relative volume, which is the raw volume divided by the mean value of the nuclear volume at each stage. Finally, we normalized the durations of each track by calculating the relative covered volume per second (Figure 4F).

Mean Cyst number estimation

To generate *y,w^{1118} hs-FLP; FRT40A-GFP/ FRT40A-mRFP* flies, we crossed *y,w^{1118} hs-FLP; FRT40A-GFP with y,w hs-FLP; FRT40A-mRFP*. The resulting larvae were subjected to 1 hour heat shocks for 3 days to activate the flipase. This allows recombination at the FRT sites, to generate clones of red (homozygous mRFP), green (homozygous GFP) or green and red (mRFP / GFP) colors. Mosaic adult ovaries and testes having red, green or green and red cells, make it easier to count the number of cysts at different stages. We used the mean cyst number to calculate cell cycle length.

Cell cycle length estimation

To determine the cell cycle length of germ cells in males and females we used w1118; *svv::GFP; tmod::GFP* flies. Here *tmod::GFP* served as a fusome marker and *svv::GFP,* which associates with centromeres during mitosis, allowed counting the number of mitosis. For example, 1 testis with ± 10.4 GSCs, we calculated the total amount of time GSCs were imaged (10.4 GSC x 15.8 hours) and divided it by the total number of GSC divisions observed during that time (8 cell divisions) to obtain a mean cell cycle duration for GSCs of 20.6 hours (10.4 x 15.8/8). We calculated similarly the mean cell cycle time for each stage (Figure 6A-B) (15). The length of each movie was determined by the last germline mitosis observed at any stage.

To measure the effect of shRNA lines on cell cycle length, *svv::GFP/CyO; bamGal4/TM3Ser* females were crossed shRNA males. The resulting progenies of *svv::GFP; bam>shRNA* females were dissected in hydrogel, as described above. Live-images were analyzed as above.

FIGURE S1

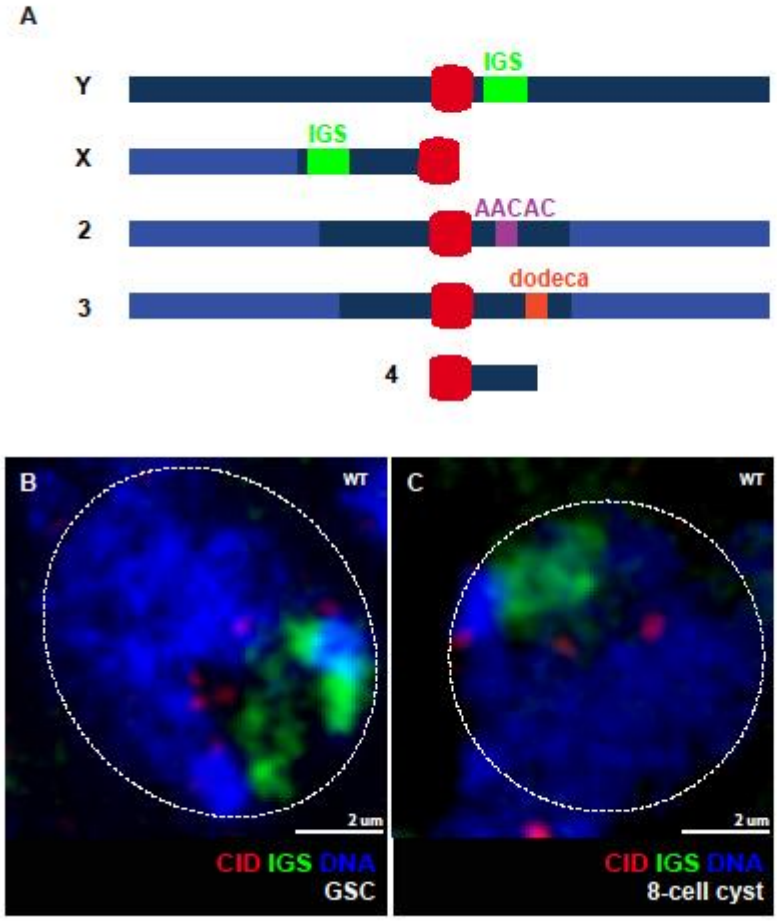

Fig. S1. (A) Drosophila chromosomes and targets of FISH probes. Heterochromatin is denoted in dark blue, IGS region in green, probes AACAC in purple and dodeca in orange, and centromeres in red. (B, C) Confocal Z-section projections of a wild-type testis stained for chromosome rDNA (IGS probe, green), centromere (CID, red) and DNA (DAPI, blue). (B) GSC shows a broad and diffuse IGS signal next to CID foci. (C) 8-cell cyst shows broad and diffuse IGS signal next to CID foci. Dotted lines surround nuclei. Scale bar is 2 μm.

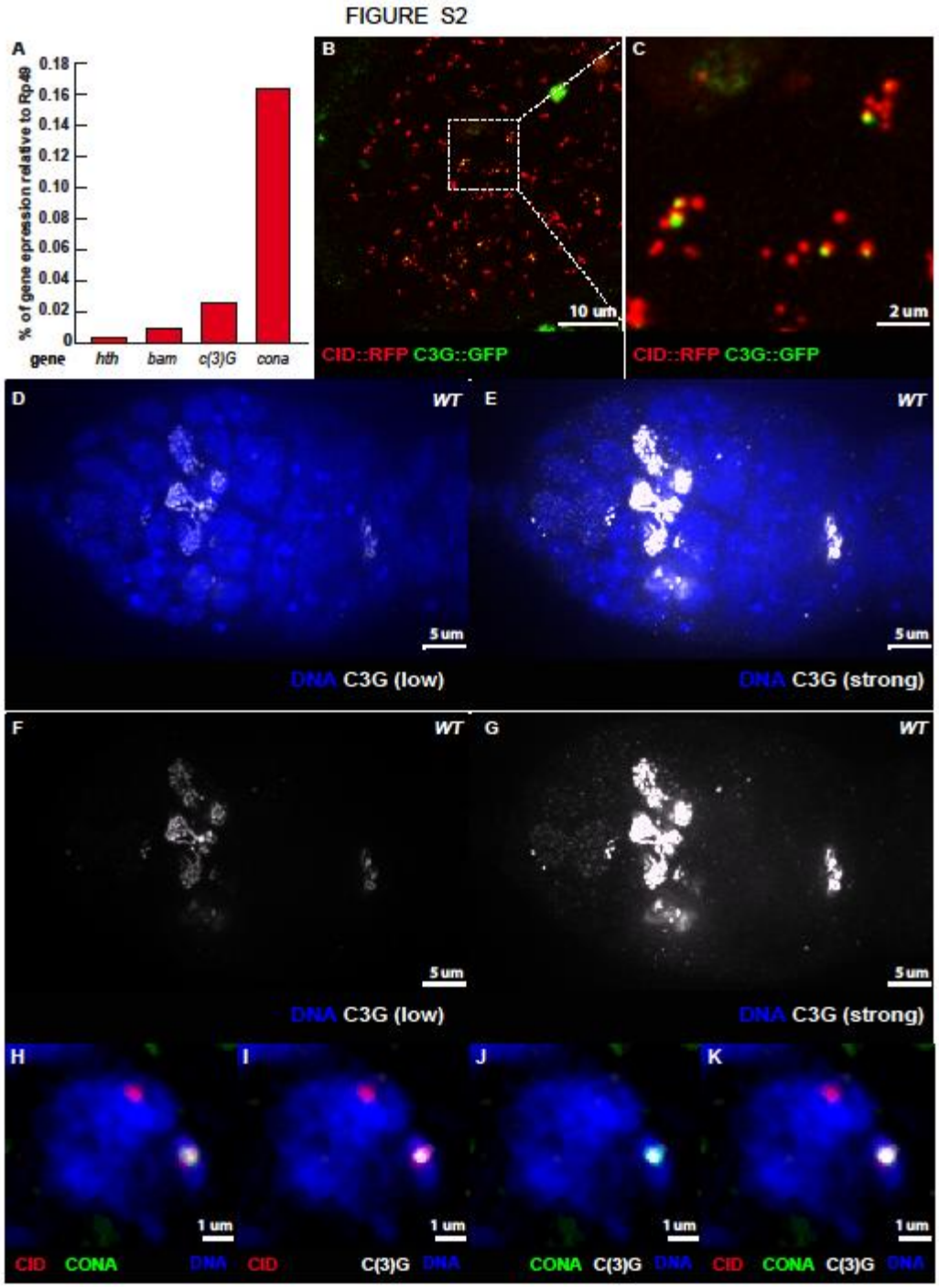

Fig. S2. (A) Real-time qPCR of *hth*, *bam, c(3)G,* and *cona.* Relative amount of gene expression with respect to *rp49* in testis. (B) Z-section projections obtained by live-imaging of a testis expressing CID::RFP (red) and C(3)G::GFP (green). (C) Magnified view of a CID::RFP–C(3)G::GFP association corresponding to region outlined in (B). (D-G) Confocal Z-section projections of a wild-type germarium stained for C(3)G (white) and DNA (DAPI, blue). Low signal

panels (D, F) show the classical rod pattern of synaptonemal complex in meiotic region, and High signal panels (E,G) reveals C(3)G nuclear localization in the mitotic region. Scale bar in B is 10 µm, C is 2 µm, D-G is 5 µm.

(H-K) Confocal Z-section projections of a male mitotic germ cell stained for centromere (CID, red), C(3)G (Grey), CONA (Green) and DAPI (Blue). Scale bar is 1 µm.

Figure S3

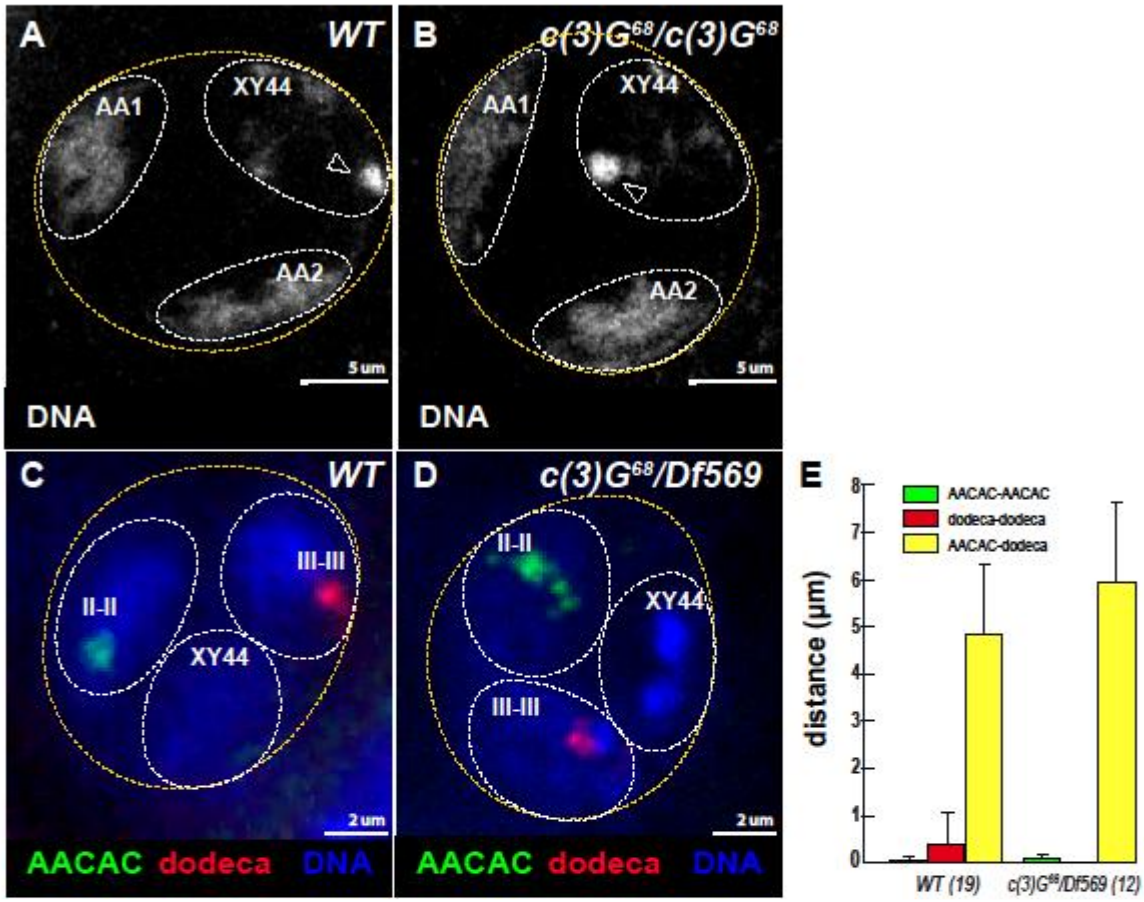

Fig. S3**.** (A,B) Confocal Z-section projections of late spermatocyte nucleus (S5-S6) in wild-type (A) and *c(3)G^{68}/c(3)G^{68}* (B) testes stained for DNA (DAPI, Grey). The nucleus frontier is indicated by yellow dashed line, the three chromosome territories are indicated (white dashed lines) with the corresponding autosomes (AA1/AA2) territories and the XY44 territory, containing the nucleolus (arrowhead). (C,D) Confocal Z-section projections of early spermatocyte nucleus (S2-S3) in wild-type (C) and *c(3)G^{68}/c(3)GDf569* (D) testes stained for chromosome II centromeres probe (AACAC, green), chromosome III centromere probe (dodeca, red) and DNA (DAPI, Blue). (E) Graphs plot the mean distance of paired homologous chromosome II and III and the non-homologous distance between the two closest AACAC and dodeca dots in the same nucleus. The number of cells analyzed is indicated under each genotype. For distance AACAC-dodeca, p> 0.05 (two-tailed Student's t-test comparing wild type with *c(3)G^{68}/ c(3)G^{68}/c(3)GDf569*. The nucleus frontier is indicated by yellow dashed line, the three chromosome territories are indicated (white dashed lines) with the corresponding autosomes (II-II/III-III) territories and the XY44 territory, containing the nucleolus (arrowhead)Scale bar in A,B is 5 µm, C,D is 2 µm.

Figure S4

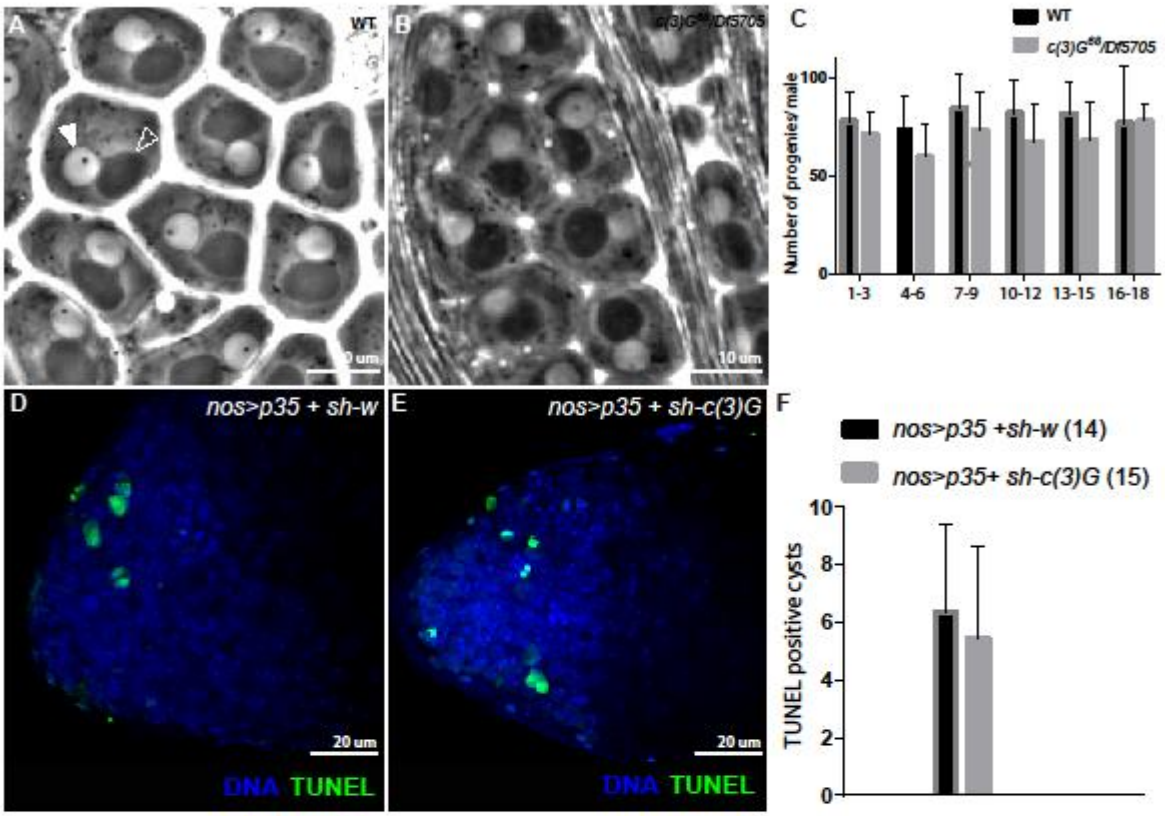

Fig. S4**.** (A,B) *c(3)G* mutants do not show postmeiotic defects. Phase-contrast micrographs of spermatids in wild-type (B) and *c(3)G*^{68}*/Df(3R)ED5705* mutants (C). Onion-stage spermatids show one haploid nucleus (arrowhead) and one mitochondrial derivative (open arrowhead) in wild-type (B) and *c(3)G*^{68}*/Df(3R)ED5705* mutants , each about the same diameter. (C) *c(3)G* mutant males do not show reduced fertility. Single *c(3)G*^{68}*/Df(3R)ED5705* males were crossed with two virgin *w*^{1118} females. Every 3 days, males were transferred to a new vial with two new virgin *w1118* females. The number of adult flies eclosed from each vial was scored. *w*^{1118} *is* the WT control. (D-F) *c(3)G* mutants do not show increase germline cell death in the premeiotic region. Apical tips of *nos>p35 + sh-w* (D) and *nos>p35 + sh-c(3)G* testes with stained nuclei (DAPI; blue) and fragmented DNA (TUNEL; green). (F) Mean number of TUNEL positive spermatogonial cysts per testis in *nos>p35 + sh-w* and *nos>p35 + sh-c(3)G*. p=0.4 (two-tailed Student's t-test comparing wild type with *c(3)G*^{68}*/Df(3R)ED5705).* Scale bar in B,C is 10 μm, D,E is 20 μm.

FIGURE S5

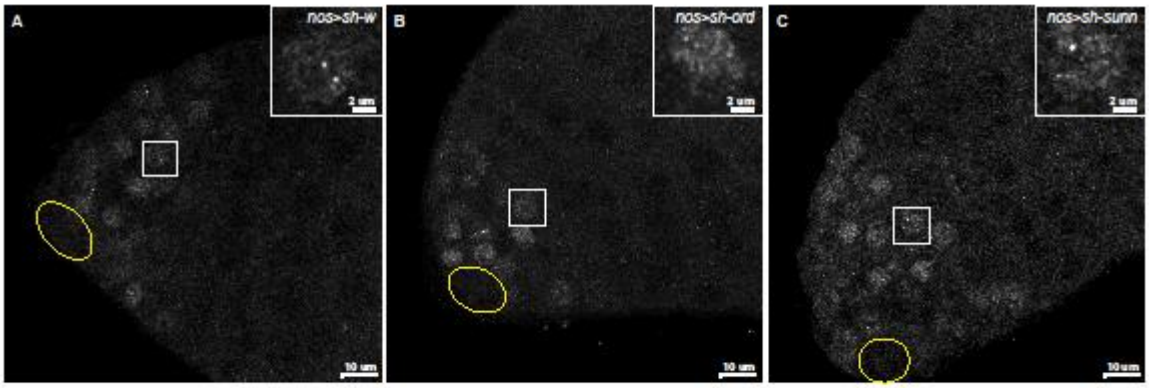

Fig. S5**.** (A-C) Confocal Z-section projections of *nos>sh-white* (A) *nos>sh-ord* (B) and *nos>sh-sunn* (C) testes stained for C(3)G (grey). The hub is marked by the yellow circle. Inserts in A-C show magnified nuclei corresponding to outlined nuclei. Scale bars in A-C are 10 μm and inserts are 2 μm.

FIGURE S6

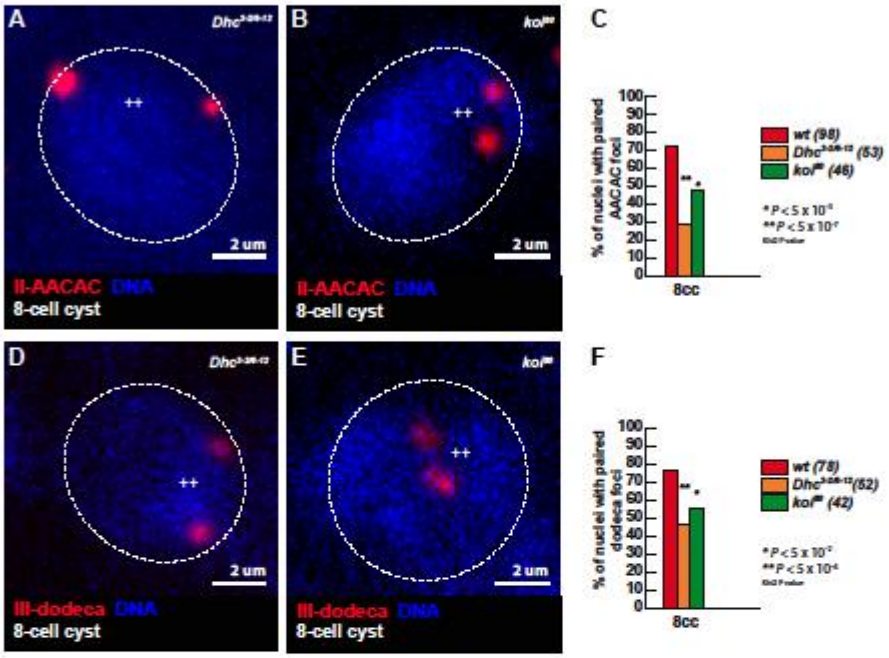

Fig. S6. **(**A,B) Projection of Z-sections obtained by confocal microscopy of *Dhc*$^{3-2}$/*Dhc*$^{6-12}$ (A) or *koi*^{80}/*koi*^{80} (B) testes stained for AACAC (red) and DNA (blue). A nucleus of an 8-cell cyst (8cc), surrounded by dotted lines, display two foci separated by a distance of ≥0.7 µm (++) indicating unpaired centromeres. Scale bar is 2 µm. (C) Percentage of paired chromosomes II in 8cc using the AACAC probe in wild-type (*wt*), *Dhc*$^{3-2}$/*Dhc*$^{6-12}$ or *koi*^{80}/*koi*^{80} fixed testes. Chromosome II centromeres are considered paired when the distance between the 2 foci is ≤0.7 µm. The number of analyzed cells is indicated next to each genotype. * p≤5x10^3, ** ≤ 5x10^7 (khi2 test comparing wild-type with *Dhc*$^{3-2}$/*Dhc*$^{6-12}$ or *koi*^{80}/*koi*^{80}. (D, E) Projection of Z-sections obtained by confocal microscopy of *Dhc* $^{3-2}$/*Dhc* $^{6-12}$ (D) or *koi* ^{80}/*koi* ^{80} (E) testes stained for dodeca (red) and DNA (blue). One nucleus of an 8-cell cyst (8cc), surrounded by dotted lines, displays two foci separated by a distance of ≥ 0.7 µm (++) indicating unpaired centromeres. Scale bar is 2 µm. (F) Percentage of paired chromosomes II in 8cc using the dodeca probe in *wt*, *Dhc*$^{3-2}$/*Dhc*$^{6-12}$ or *koi*^{80}/*koi*^{80} fixed testes. Chromosome III centromeres are considered paired when the distance between the 2 foci is ≤0.7 µm. The number of analyzed cells is indicated next to each genotype. * p≤5x10^2, ** ≤5x10^4 (khi2 test comparing wild-type with *Dhc*$^{3-2}$/*Dhc*$^{6-12}$ or *koi*^{80}/*koi*^{80}).

FIGURE S7

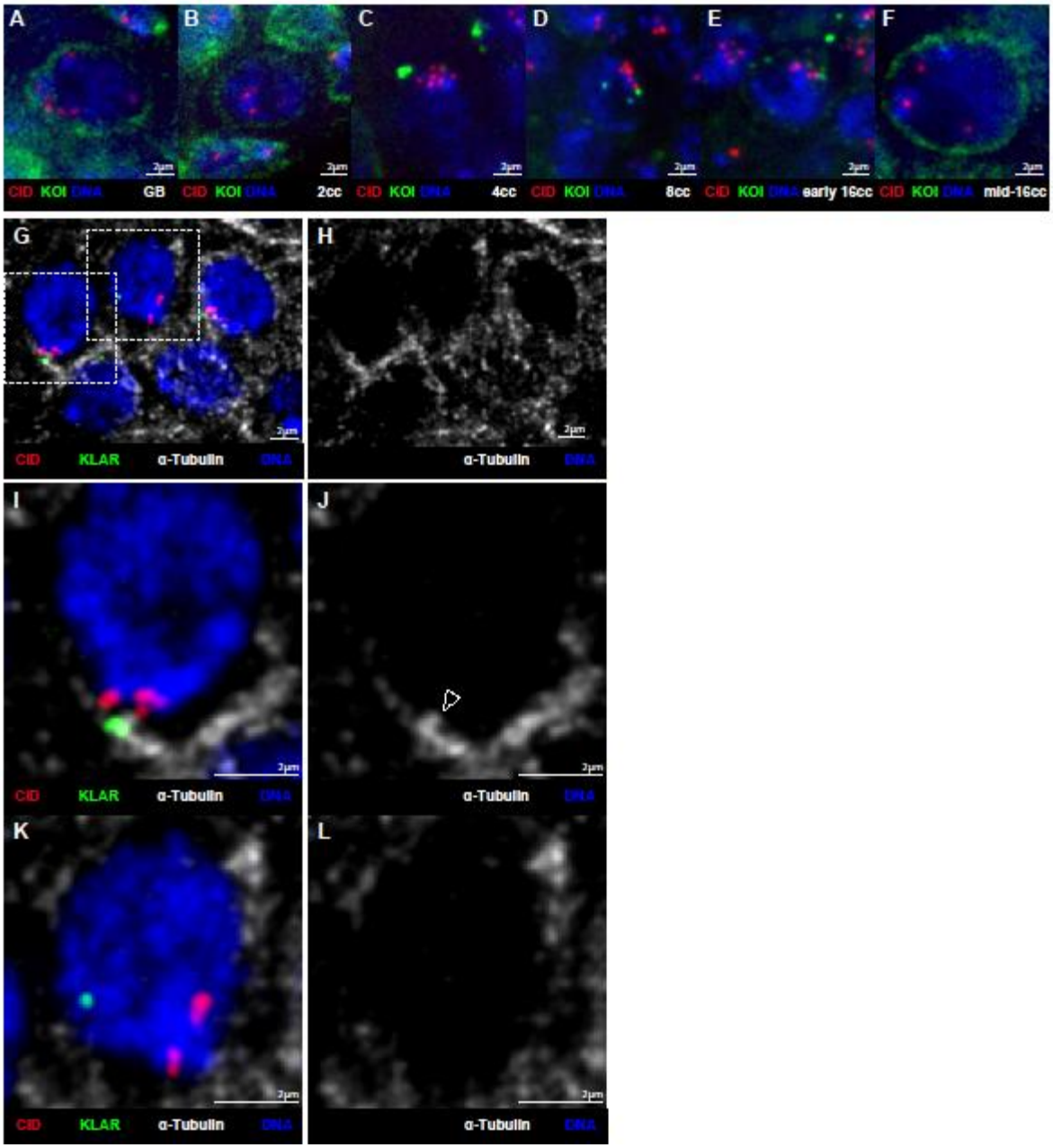

Fig. S7**.** (A-F) Projections of Z-sections obtained by confocal microscopy of wild-type *koi::GFP* nuclei stained for CID (red) and DNA (DAPI, blue). (A) Gonioblast, GB; (B) 2-cell cyst, 2cc; (C) 4-cell cyst, 4cc; (D) 8-cell cyst, 8cc; (E) early 16-cell cyst, 16cc; (F) mid 16-cell cyst, 16cc. (G-L) Projections of Z-sections obtained by confocal microscopy of wild-type *8cc* nuclei stained for CID (red), Klar (Green) , α-tubulin (Grey) and DNA (DAPI, blue). . Inserts in G are magnified in I-L. Arrowhead points to a tubulin bundle colocalizing with Klar in I,J but not K,L. Scale bars are 2 µm.

FIGURE S8

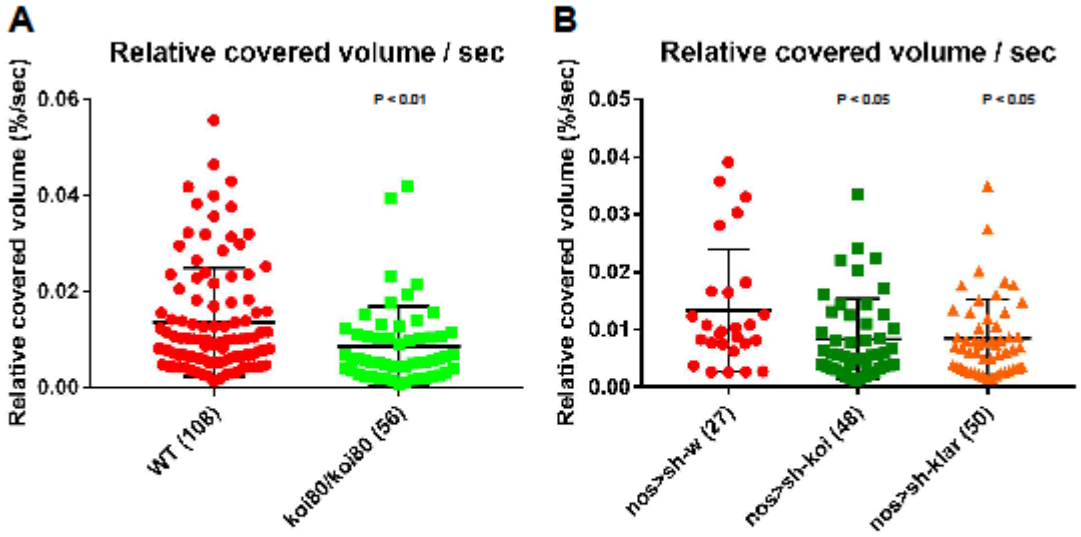

Fig. S8**.** Centromere dynamic rotations in 8-cell cysts is reduced in LINC complex mutant males. (A) Relative covered volume per second in 8-cell cysts nuclei of wild type (WT) and Klaroid (*koi*^{80} / *koi*^{80}) mutant (mean ± s.d., Mann-Whitney U-test p<0.01; WT: n=108 centromeric foci; *koi*^{80} / *koi*^{80}: n= 56 centromeric foci). (B) Relative covered volume per second in 8-cell cysts nuclei in control *nos>sh-w*; *nos>sh-koi; nos>sh-klar*. (mean ± s.d., Mann-Whitney U-test p<0.05; *nos>sh-w*: n=27 centromeric foci; *nos>sh-koi*: n= 48 centromeric foci; *nos>sh-klar* n=50 centromeric foci).

FIGURE S9

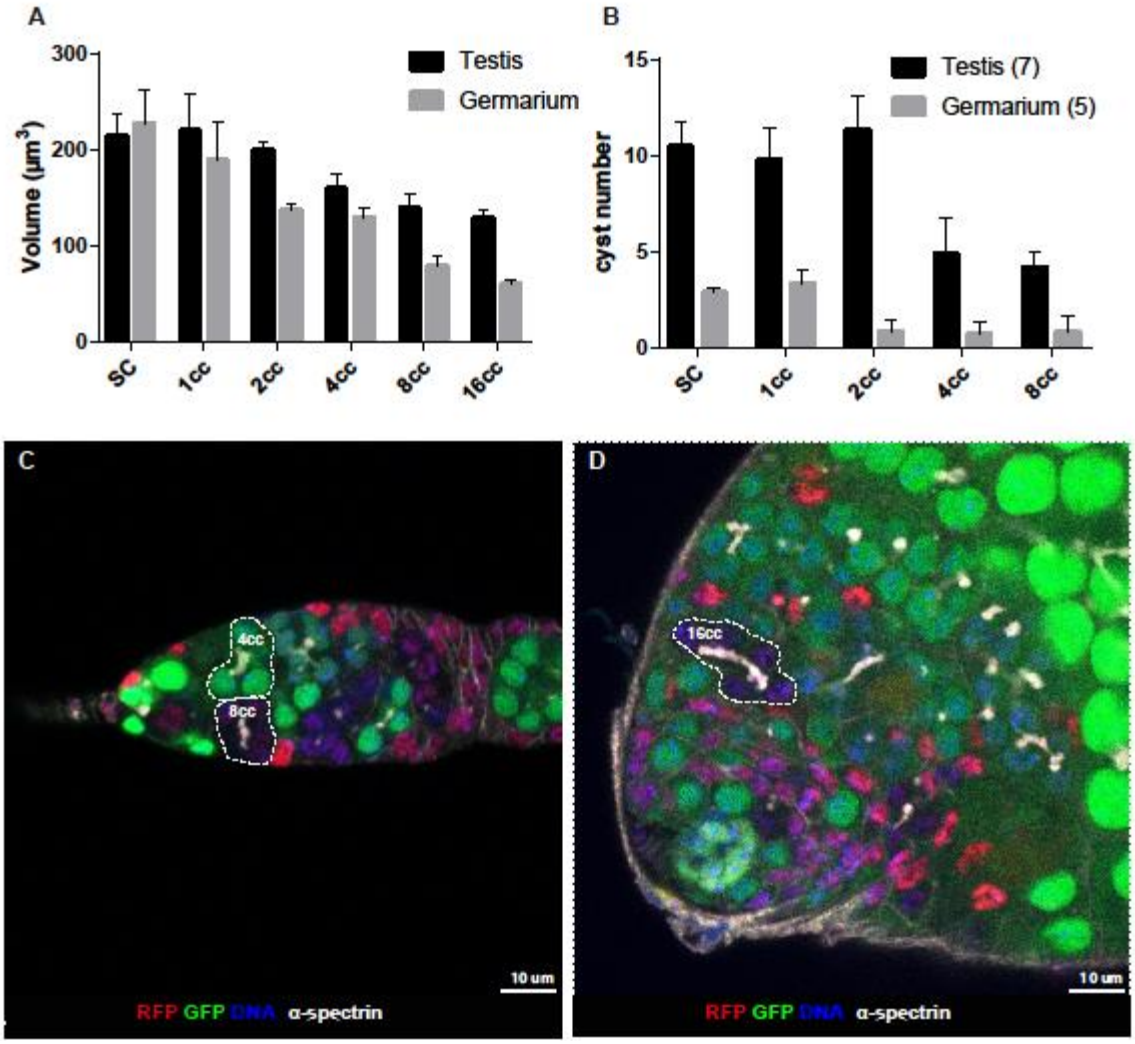

Fig. S9. (A) Mean nuclear volume for each developmental stage obtained by live-imaging Nup::GFP/+; CID::RFP/+ germarium and testis. For each nucleus, the longest (D) and the smallest diameter (d) were determined by measuring the distance between two diametrically opposed Nup::GFP signals on projected images along the x-y axis. The height of the nucleus (h) was determined from z-series starting from the first Nup foci detected until the last one. Nuclear volume (μm^3) was calculated using the formula: $V= 4 \times D \times d \times h \times \pi/3$. The number of analyzed nuclei (n) is indicated below each stage. Values and error bars are the mean ±SD. (B) Average number of cysts per stage in a testis (n = 7) and ovary (n = 15) SC: Stem Cell; 1 cc: Gonioblast (testis) or Cystoblast (Ovary); 2cc: 2 cell-cyst; 4cc: 4 cell cyst; 8cc: 8 cell-cyst. (C, D) Selected projections from *yw1118 hs-FLP; FRT40A-GFP/FRT40A-mRFP* used to generate mosaic germarium (C) and testis (D) stained for GFP (green), RFP (red), fusome (α–spectrin, white) and DNA (DAPI, blue). Counting the number of cysts at each stage is facilitated by having red, green or both color cysts. Scale bars are 10 µm.

Figure S10

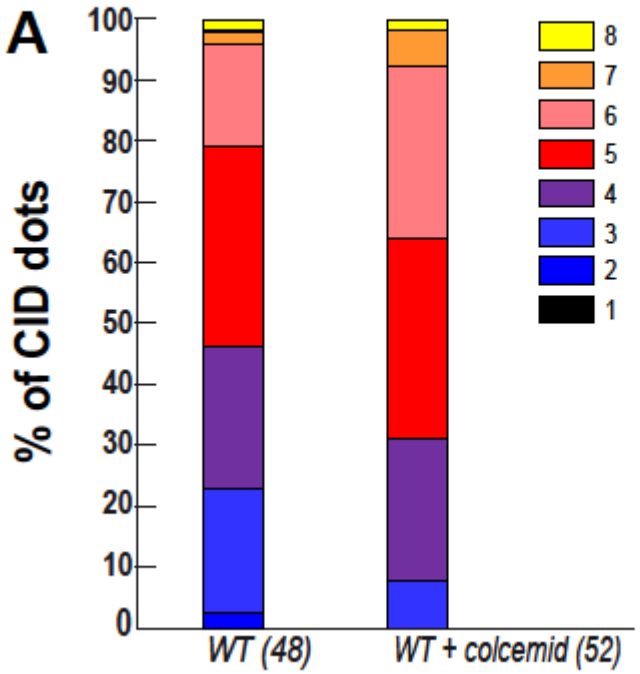

Fig. S10. Distribution of CID dots in wild type (WT) and wild type colcemid treated (WT + colcemid) testes. Each color corresponds to the number of CID dots per nucleus in 8-cell cysts. The number of nuclei analyzed (n).

Table S1. NDJ in *SC* mutant males

A. Sex chromosome NDJ Frequencies :

	Sperm genotype					
	X	Y	XY	O	Nc	% NDJ
Paternal genotype :						
+/+	194	164	1	1	360	0.55
c(3)G^{68}/Df569	217	222	1	0	440	0.22

w/BsYy+ males with indicated third chromosome were crossed to *w* females.
Nc is total number of progeny scored
% NDJ is 100 x XY + O/Nc

B. 2nd chromosome NDJ Frequencies :

	Sperm genotype		
	Diplo-2	Nullo-2	F1/n
Paternal genotype :			
+/+	0	0	0
c(3)G^{68}/Df5705	0	0	0
cona^{A12}/cona^{4973}	0	0	0

Males with indicated third chromosome were crossed to *C(2)EN b^{1} pr^{1}* females
F1/n is the frequency of NDJ/total number of males crossed (20)

Table S2. 2nd chromosome NDJ in *c(3)G* combined with different meiotic mutant RNAi lines

	Sperm genotype		
	Diplo-2	Nullo-2	F1/n males
Paternal genotype :			
nos>sh-c(3)G	2	0	0.05
nos>sh-c(3)G+ sh-tef	1	1	0.1
nos>sh-tef	0	0	0
nos>sh-c(3)G+ sh-mnm(32)	45	42	5.8
nos>sh-mnm(32)	78	53	6.55
nos>sh-c(3)G+ sh-ord	59	65	8.27
nos> sh-ord	85	68	7.65
nos>sh-c(3)G+ sh-sunn	66	44	5.50
nos> sh-sunn	59	54	5.65

Males with indicated chromosome were crossed to *C(2)EN b pr* females. F1/n is the frequency of NDJ/total number of males crossed (20). (32) is RNAi lines HMS00795.

Table S3. 2nd chromosome NDJ Frequencies in *c(3)G; ord* mutant

	Sperm genotype		
	Diplo-2	Nullo-2	F1/n males
Paternal genotype :			
ord^{10}/+ ; c(3)G^{68}/Df569	0	0	0
ord^{10}/+ ;+/Df569	1	0	0.05
+/+ ;+/Df569	1	1	0.1
ord^{10}/+ ;+/+	0	0	0

Males with indicated genotypes were crossed *to C(2)EN b pr* females. F1/n is the frequency of NDJ/total number of males crossed (20)

Table S4. Sex chromosome NDJ in *c(3)G* combined with different meiotic mutant RNAi lines

	Sperm genotype					
Paternal genotype :	X	Y	XY	O	Nc	%NDJ
nos>sh-c(3)G	615	585	7	14	1221	1.7
nos>sh-c(3)G+ sh-mnm(32)	440	419	158	266	1283	33
nos>sh-mnm(32)	407	384	182	304	1277	38
nos>sh-c(3)G+ sh-mnm(33)	851	813	42	176	1882	11.6
nos> sh-mnm(33)	753	651	18	192	1614	13

w/BsYy+ males with indicated genotypes were crossed to *w* females. (32) and (33) are RNAi lines HMS00795, HMS00849, respectively.
Nc is total number of progeny scored
% NDJ is 100 x XY + O/Nc

Table S5. NDJ in *koi* mutants

A. Sex chromosome NDJ Frequencies

	Sperm genotype					
	X	Y	XY	O	Nc	%NDJ
Paternal genotype :						
koi^{80}/koi^{80}	1012	983	6	8	2009	0.7
+/+	512	491	5	4	1012	0.9

w/BsYy+ males with indicated second chromosome were crossed to *w* females.
Nc is total number of progeny scored
% NDJ is 100 x XY + O/Nc

B. 2nd chromosome NDJ Frequencies

	Sperm genotype		
	Diplo-2	Nullo-2	F1/n males
Paternal genotype :			
+/+	0	0	0
koi^{80}/koi^{80}	0	0	0

Males with indicated third chromosome were crossed to *C(2)EN b pr* females. F1/n is the frequency of NDJ/total number of males crossed (20).

Table S6. Quantification

Figure 1E : *GSC* (66) ; *GB* (32) ; *2cc* (29) ; *4cc* (44) ; *8cc* (48) ; *16cc* young (29) ; *16cc* mid (12) ; S4-S5 (46) from 14 testes.

Figure 1F : *GSC* (22) ; *GB* (16) ; *2cc* (29) ; *4cc* (41) ; *8cc* (45) ; *16cc* young (29) ; *16cc* mid (12) ; *16cc* old (31) from 14 testes.

Figure 2C : *GSC* (29 ; 4 testes) ; *GB* (17, 11 testes) ; *2cc* (37 ; 3 testes) ; *4cc* (28 ; 7 testes) ; *8cc* (98 ; 10 testes) ; *16cc* (38 ; 2 testes).

Figure 2F : *GSC* (28; 4 testes) ; *GB* (19, 11 testes) ; *2cc* (28; 3 testes) ; *4cc* (25; 7 testes) ; *8cc* (78; 10 testes) ; *16cc* (37; 2 testes).

Figure 3G : *wt (48 ; 10 testes) ; c(3)G $^{Df569/EP}$ (46 ; 6 testes) ; c(3)G $^{Df5705/EP}$ (44 ; 6 testes) ; c(3)G $^{Df569/1}$ (42 ; 6 testes) ; c(3)G $^{Df5705/1}$ (43 ; 6 testes) ; cona $^{04903/A12}$ (60 ; ?? testes)* .

Figure 3H : *wt (45 ; 14 testes) ; c(3)G $^{68/68}$ (38 ; 10 testes) ; cona $^{04903/A12}$ (54 ; 15 testes)*.

Figure 3K : *wt (98 ; 10 testes) ; c(3)G $^{Df569/68}$ (50 ; 7 testes) ; cona $^{f04903/A12}$ (54 ; 7 testes).*

Figure 3N : *wt (78 ; 10 testes) ; c(3)G $^{Df569/68}$ (48; 7 testes) ; cona $^{f04903/A12}$ (51; 7 testes).*

Figure 4E, F : *GSC* (34 tracks ; 7 *GSC* ; 5 testes) ; *GB* (46 tracks; 7 *GB* ; 2 testes) ; *2cc* (35 tracks ; 7 *2cc* ; 4 testes) ; *4cc* (57 tracks ; 12 *4cc* ; 4 testes) ; *8cc* (108 tracks ; 25 *8cc* ; 7 testes) ; *16cc* (46 tracks ; 4 *16cc* ; 2 testes).

Figure 4G : WT Males (108 tracks ; 28 *8cc* ; 7 testes); WT Females (35 tracks ; 18 *8cc* ; 6 germaria).

Figure 4H : WT (108 tracks ; 28 *8cc* ; 7 testes); WT + Colcemid (50 tracks ; 3 testes); *Dhc64$^{3-2/6-12}$* (39 tracks ; 13 *8cc* ; 5 testes) .

Figure 4K : *wt (47 8cc ; 8 testes) ; wt+colcemid (56 8cc ; 6 testes) ; Dhc64$^{3-2/6-12}$ (26 8cc ; 3 testes).*

Figure 50 : *wt (48 8cc ; 10 testes) ; klar $^{marb-CD4/marb-CD4}$ (63 8cc ; 7 testes) ; koi$^{80/80}$ (45 8cc ; 8 testes).*

Figure 6 : A, 18 testes *svv::GFP/+ ;tmod::GFP/+* for 254h total movies; B, 26 germaria *svv::GFP/+ ;tmod::GFP/+* for 235h total movies.

Figure 6C : *svv::GFP/+ ; bam>sh-w* (73 germaria ; 185h total movies) ; *svv::GFP/+ ; bam>sh-CycB* (37 germaria ; 257h total movies) ; *svv::GFP/+ ; bam>sh-cdc2/CDK1* (37 germaria ; 211h total movies) ; *bam>sh-twine* (29 germaria ; 182h total movies).

Figure 6F : *w (54 8cc; ??germaria); koi$^{80/80}$; bam>sh-w (34 8cc ; 5 germaria) ; koi$^{80/80}$; bam>sh-CycB (37 8cc ; 4 germaria) ; koi$^{80/80}$; bam>sh-cdc2/CDK1 (29 8cc ; 4 germaria) ; koi$^{80/80}$; bam>sh-twine (45 8cc ; 6 germaria).*

Figure S3A,B : *WT* (57 cells, 7 testes), *c(3)G^{68}/c(3)G^{68}* (57 cells, 6 testes).

Figure S3E : *WT* (34 cells, 13 testes), *c(3)G^{68}/Df569* (28 cells, 12 testes).

Figure S4A : : *WT* males (n=19), *c(3)G^{68}/Df(3R)ED5705* males (n=20).

Figure S4F : *nos>p35+sh-w* : 14 testes, *nos>p35+sh-c(3)G* : 15 testes.

Figure S6 : *WT* (48 *8cc*, 8 testes), *WT+ colcemid* (52 *8cc*, 6 testes).

Figure S8A : *WT* (108 tracks ; 28 *8cc* ; 7 testes) ; koi^{80}/koi^{80} (56 tracks ; 22 *8cc* ; 4 testes).

Figure S8B : *nos>sh-w* (27 tracks ; 10 *8cc* ; 3 testes) ; *nos>sh-koi* (48 tracks ; 9 *8cc* ; 3 testes) ; *nos>sh-klar* (50 tracks ; 14 *8cc* ; 3 testes).

Figure S9C : *wt* (98 *8cc*, 10 testes), $Dhc64^{3\text{-}2/6\text{-}12}$ (53 *8cc*, 7 testes), $koi^{80/80}$ (46 *8cc*, 6 testes).

Figure S9F : *wt* (78 *8cc*, 10 testes), $Dhc64^{3\text{-}2/6\text{-}12}$ (52 *8cc*, 7 testes), $koi^{80/80}$ (42 *8cc*, 6 testes).

Figure S10A : Testis (10 *GSC*, 10 *GB*, 10 *2cc*,11 *4cc*, 9 *8cc*, 10 *16cc*), Germarium (7 *GSC*, 5 *CB*, 4 *2cc*, 5 *4cc*, 6 *8cc*).

Figure S10B : Testes, 7; Germaria, 5.

Movie S1 (separate file). Dynamics of centromeres and telomeres in the mitotic region of a testis. Time lapse microscopy (spinning disc) of a testis expressing the centromere marker CID::RFP (red) and the telomere marker HIPHOP::GFP (green) shows that both centromeres and telomeres in a mitotic region germ cell are found dispersed along the entire nucleus (circle). Frames were taken every 10 seconds. The video is shown at 7 frames/s (MPEG4).

Movie S2 (separate file). Dynamics of centromere clusters in the mitotic region of a testis. Time lapse microscopy (spinning disc) of a testis expressing the centromere marker CID::RFP (red) and the fusome marker MUD::GFP (green). One germinal stem cell (GSC) is identified (open arrow) by its position close to the hub (yellow circle). Two nuclei of an 8-cell cyst (8cc), whose cells are linked by a branched-shaped fusome, demonstrating that they are from the same cyst. Arrows point towards rotating centromeres cluster in an 8cc. Frames were taken every 10 seconds. The video is shown at 7 frames/s (MPEG4).

Movie S3 (separate file). Centromere dynamics in wild-type GSC. Live time lapse microscopy (spinning disc) of a testis expressing the centromere marker CID::RFP (red). White circle marks the nucleus. Frames were taken every 10 seconds. The movie is shown at 7 frames/s (MPEG4).

Movie S4 (separate file). Centromere dynamics in wild-type 8-cell cyst. Live time lapse microscopy (spinning disc) of a testis expressing the centromere marker CID::RFP (red). White circle marks the nucleus. Frames were taken every 10 seconds. The movie is shown at 7 frames/s (MPEG4)

Movie S5 (separate file). CID-RFP and C(3)G-GFP are in close proximity in testis. Live time lapse microscopy (spinning disc) of a testis expressing the centromere marker CID::RFP (red) and the C(3)G::GFP (green). Frames were taken every 30 seconds. The movie is shown at 7 frames/s (MPEG4).

Movie S6 (separate file). CID-RFP and CONA-Venus are in close proximity in testis. Live time lapse microscopy (spinning disc) of a testis CID::RFP; nos>Cona::Venus expressing the centromere marker CID::RFP (red) and the CONA::Venus (green). Frames were taken every 20 seconds. The movie is shown at 7 frames/s (MPEG4).

Movie S7 (separate file). Colcemid treatment leads to inhibition of CID foci dynamics in 8-cell cysts. Live time lapse microscopy (spinning disc) of a colcemid-treated testis expressing the centromere marker CID::RFP. White circle marks the nucleus. Frames were taken every 10 seconds. The movie is shown at 7 frames/s (MPEG4).

Movie S8 (separate file). *Dynein* loss of function in *Dhc64C* $^{3-2}$*/Dhc64C* $^{6-12}$ mutant leads to inhibition of CID foci dynamics in 8-cell cysts. Live time lapse microscopy (spinning disc) of a *Dhc64C* $^{3-2}$*/Dhc64C* $^{6-12}$ mutant testis expressing the centromere marker CID::RFP. White circle marks the nucleus. Frames were taken every 10 seconds. The movie is shown at 7 frames/s (MPEG4).

SI References

1. S. L. Page et al., Corona is required for higher-order assembly of transverse filaments into full-length synaptonemal complex in Drosophila oocytes. PLoS Genet 4, e1000194 (2008).
2. M. P. Kracklauer, S. M. Banks, X. Xie, Y. Wu, J. A. Fischer, Drosophila klaroid encodes a SUN domain protein required for Klarsicht localization to the nuclear envelope and nuclear migration in the eye. Fly (Austin) 1, 75-85 (2007).
3. M. Technau, S. Roth, The Drosophila KASH domain proteins Msp-300 and Klarsicht and the SUN domain protein Klaroid have no essential function during oogenesis. Fly (Austin) 2, 82-91 (2008).
4. J. Gepner et al., Cytoplasmic dynein function is essential in Drosophila melanogaster. Genetics 142, 865-878 (1996).
5. S. E. Bickel, D. W. Wyman, T. L. Orr-Weaver, Mutational analysis of the Drosophila sister-chromatid cohesion protein ORD and its role in the maintenance of centromeric cohesion. Genetics 146, 1319-1331 (1997).
6. M. Schuh, C. F. Lehner, S. Heidmann, Incorporation of Drosophila CID/CENP-A and CENP-C into centromeres during early embryonic anaphase. Curr Biol 17, 237-243 (2007).
7. F. Bosveld et al., Epithelial tricellular junctions act as interphase cell shape sensors to orient mitosis. Nature 530, 495-498 (2016).
8. J. Mathieu et al., Aurora B and cyclin B have opposite effects on the timing of cytokinesis abscission in Drosophila germ cells and in vertebrate somatic cells. Dev Cell 26, 250-265 (2013).
9. D. V. Lighthouse, M. Buszczak, A. C. Spradling, New components of the Drosophila fusome suggest it plays novel roles in signaling and transport. Dev Biol 317, 59-71 (2008).
10. K. R. Katsani, R. E. Karess, N. Dostatni, V. Doye, In vivo dynamics of Drosophila nuclear envelope components. Mol Biol Cell 19, 3652-3666 (2008).

11. R. Dubruille et al., Specialization of a Drosophila capping protein essential for the protection of sperm telomeres. Curr Biol 20, 2090-2099 (2010).
12. K. J. Livak, T. D. Schmittgen, Analysis of relative gene expression data using real-time quantitative PCR and the 2(-Delta Delta C(T)) Method. Methods 25, 402-408 (2001).
13. N. Christophorou, T. Rubin, J. R. Huynh, Synaptonemal complex components promote centromere pairing in pre-meiotic germ cells. PLoS Genet 9, e1004012 (2013).
14. K. Burnett, E. Edsinger, D. R. Albrecht, Rapid and gentle hydrogel encapsulation of living organisms enables long-term microscopy over multiple hours. Commun Biol 1, 73 (2018).
15. X. R. Sheng, E. Matunis, Live imaging of the Drosophila spermatogonial stem cell niche reveals novel mechanisms regulating germline stem cell output. Development 138, 3367-3376 (2011).